Received: 7 January 2021 | Revised: 5 March 2021 | Accepted: 8 March 2021

DOI: 10.1002/hbm.25414

RESEARCH ARTICLE

WILEY

Spatial correlation maps of the hippocampus with cerebrospinal fluid biomarkers and cognition in Alzheimer's disease: A longitudinal study

Guodong Liu[1] | **Chaoqiang Liu**[1] | **Anqi Qiu**[1,2,3,4] | **the Alzheimer's Disease Neuroimaging Initiative**

[1]Department of Biomedical Engineering, National University of Singapore, Singapore, Singapore

[2]The N.1 Institute for Health, National University of Singapore, Singapore, Singapore

[3]Smart Systems Institute, National University of Singapore, Singapore, Singapore

[4]Department of Biomedical Engineering, Johns Hopkins University, Baltimore, Maryland

Correspondence
Anqi Qiu, Department of Biomedical Engineering, National University of Singapore, 4 Engineering Drive 3, Block E4 #04-08, Singapore 117583, Singapore.
Email: bieqa@nus.edu.sg

Funding information
Singapore Ministry of Education and NUS Institute of Data Science; National Research Foundation, Singapore, Grant/Award Number: AISG-GC-2019-002

Abstract

This study is an observational study that takes the existing longitudinal data from Alzheimer's disease Neuroimaging Initiative to examine the spatial correlation map of hippocampal subfield atrophy with CSF biomarkers and cognitive decline in the course of AD. This study included 421 healthy controls (HC), 557 patients of stable mild cognitive impairment (s-MCI), 304 Alzheimer's Disease (AD) patients, and 241 subjects who converted to be AD from MCI (c-MCI), and 6,525 MRI scans in a period from 2004 to 2019. Our findings revealed that all the hippocampal subfields showed their accelerated atrophy rate from cognitively normal aging to stable MCI and AD. The presubiculum, dentate gyrus, and fimbria showed greater atrophy beyond the whole hippocampus in the HC, s-MCI, and AD groups and corresponded to a greater decline of memory and attention in the s-MCI group. Moreover, the higher atrophy rates of the subiculum and CA2/3, CA4 were also associated with a greater decline in attention in the s-MCI group. Interestingly, patients with c-MCI showed that the presubiculum atrophy was associated with CSF tau levels and corresponded to the onset age of AD and a decline in attention in patients with c-MCI. These spatial correlation findings of the hippocampus suggested that the hippocampal subfields may not be equally impacted by normal aging, MCI, and AD, and their atrophy was selectively associated with declines in specific cognitive domains. The presubiculum atrophy was highlighted as a surrogate marker for the AD prognosis along with tau pathology and attention decline.

KEYWORDS
cognitive function, CSF tau pathology, hippocampal subfields, longitudinal study, MRI, the onset of AD

Data used in preparation of this article were obtained from the Alzheimer's Disease Neuroimaging Initiative (ADNI) database (adni.loni.usc.edu). As such, the investigators within the ADNI contributed to the design and implementation of ADNI and/or provided data but did not participate in analysis or writing of this report. A complete listing of ADNI investigators can be found at: http://adni.loni.usc.edu/wp-content/uploads/how_to_apply/ADNI_Acknowledgement_List.pdf.

1 | INTRODUCTION

Converging evidence suggests that hippocampal volume loss is typically considered to be a hallmark of Alzheimer's disease (AD; Gerischer et al., 2018; Lehtovirta et al., 1995; Likeman et al., 2005). Cross-sectional structural magnetic resonance imaging (MRI) studies consistently revealed a smaller hippocampal volume in patients with AD compared to cognitively normal subjects (Brunton, Ginestet, Lovestone, Muehlboeck, & Simmons, 2011; Laakso et al., 1998; Laakso et al., 2000). The hippocampal atrophy over time is accelerated in patients with AD compared to cognitively normal individuals or patients with mild cognitive impairment (MCI; Strawbridge et al., 2018). Nevertheless, the hippocampus comprises many interconnected anatomically and functionally distinct subfields (Small, Schobel, Buxton, Witter, & Barnes, 2011). It is unclear to what extent individual hippocampal subfields are centrally involved in the progression of AD and are in relation to AD pathology and cognitive decline in the course of AD.

The hippocampus is mainly divided into the subicular complex, cornu ammonis (CA1–4), and dentate gyrus (DG). The AD-related pathology of the hippocampus, such as tau pathology and amyloid-β deposits, is topologically specific to its subfields. Tau pathology affects the CA1 and DG and amyloid-β influences the CA1, subiculum, and presubiculum prior to the other hippocampal subfields (Apostolova et al., 2015; Braak & Braak, 1995). Moreover, structural MRI studies also demonstrated that the hippocampal subfields are impacted differently according to different AD stages (Adler et al., 2018). Some studies reported a lower CA1 volume in patients with MCI and AD compared with cognitively normal individuals (Adler et al., 2018; La Joie et al., 2013; Parker et al., 2019), while others found lower volumes in most of the hippocampal subfields, except the parasubiculum (Parker et al., 2019). Longitudinally, the progressive involvement of the CA1 and subiculum atrophy was observed from cognitively normal to MCI, then the atrophy was spread to the CA2 and CA3 from MCI to AD (Apostolova, Mosconi, Thompson, Green, & Leon, 2010). These findings suggested that the hippocampal subfields may not be equally impacted by MCI and AD (Apostolova et al., 2006; Braak, Alafuzoff, Arzberger, Kretzschmar, & Del Tredici, 2006; Braak & Braak, 1997; Kerchner et al., 2012; La Joie et al., 2013).

Moreover, the hippocampus plays a crucial role in episodic memory whose deficit has been implicated in AD. Interestingly, recent studies have shown that hippocampal subfields could have different functional specializations (Acsády & Káli, 2007; Aggleton & Christiansen, 2015; Broadhouse et al., 2019; Hasselmo, 2005; Hunsaker & Kesner, 2008; Nakazawa, McHugh, Wilson, & Tonegawa, 2004; Ogawa et al., 2019; Travis et al., 2014; Wan, Aggleton, & Brown, 1999). The subiculum is vital for human memory and rodent spatial learning (Aggleton & Christiansen, 2015). Rodents with subiculum lesions showed impaired spatial working memory (Aggleton & Christiansen, 2015). In contrast, the CA1 is responsible for consolidation, late retrieval, and recognition (Hunsaker & Kesner, 2008; Nakazawa et al., 2004; Wan et al., 1999). The CA3 and DG are responsible for memory encoding and early retrieval (Acsády & Káli, 2007; Hasselmo, 2005; Travis et al., 2014). Imaging research showed that the DG volume significantly correlated with a decline of verbal learning and memory in patients with MCI (Broadhouse et al., 2019). Beyond learning and memory, the subfield volumes in the CA1, the subiculum, and the DG were highly correlated with the Montreal Cognitive Assessment that is the combination of visuospatial abilities, language abilities, and short-term memory recall (Ogawa et al., 2019). Nevertheless, there is a lack of research on insights into whether atrophy within specific hippocampal subfields is correlated to the decline of specific cognitive domains in the progression from cognitively normal aging, MCI, to AD over time.

This study employed the structural MRI, CSF biomarkers, and cognitive data of the Alzheimer's Disease Neuroimaging Initiative (ADNI) over the last 15 years and examined: (a) the atrophy rate of specific hippocampal fields in cognitively stable normal individuals, patients with MCI stable over the period of the ADNI study (s-MCI), patients converted from MCI to AD (c-MCI), and patients with AD; (b) to what extent the atrophy rate of specific hippocampal subfields predicts the onset age of AD; (c) to what extent the atrophy rate of specific hippocampal subfields is associated with the AD-related pathology, including CSF amyloid-β42, t-tau, and p-tau; (d) to what extent the atrophy rate of specific hippocampal subfields is correlated with cognitive decline in the memory, language, visuospatial, and attention functions in the different stages of AD. This study provided novel evidence that links the relationship of specific hippocampal subfields with onset age of AD as well as CSF biomarkers and cognitive declines in the different stages of AD.

2 | METHODS

2.1 | Participants

Data used in the preparation of this article were obtained from the ADNI database (adni.loni.usc.edu). The ADNI was launched in 2003 as a public-private partnership, led by Principal Investigator Michael W. Weiner, MD. The primary goal of ADNI has been to test whether serial MRI, positron emission tomography, other biological markers, and clinical and neuropsychological assessment can be combined to measure the progression of MCI and early Alzheimer's disease (AD). For up-to-date information, see www.adni-info.org.

This work included subjects from ADNI1, ADNI2, and ADNIGO (n = 2099 subjects) that have been recruited since 2004. Subjects (n = 576) were excluded due to MRI image quality and missing demographic data. As a result, this study included 421 healthy controls (HC), 557 patients of stable mild cognitive impairment (s-MCI), 304 AD patients, and 241 subjects who converted to be AD from MCI (c-MCI), and 6,525 MRI scans. This study considered controls and patients with MCI whose diagnosis was stable in the period from 2004 to 2019. Each subject had 1–12 scans. Table 1 lists the clinical and demographic information of each clinical group.

2.2 | MRI data acquisition and analysis

This study included participants with 3D T1-weighted structural MRI based on ADNI (www.adni-info.org). Three-dimensional T1- weighted scans were performed on 1.5T (ADNI-1) or 3T (ADNI-2 and ADNI-GO) scanners using previously described standardized protocols at each site (Jack et al., 2008). For the 1.5T scanners, the imaging protocol was: repetition time (TR) = 2,400 ms, minimum full echo time (TE), inversion time (TI) = 1,000 ms, flip angle = 8°, field-of-view (FOV) = 240 × 240 mm^2, acquisition matrix = 256 × 256 × 170. For the 3T scanners, the imaging protocol was: TR = 2,300 ms, minimum full TE, TI = 900 ms, flip angle = 8°, FOV = 260 × 260 mm^2, acquisition matrix = 256 × 256 × 170.

FreeSurfer (version 6.0) longitudinal analysis pipeline was used to delineate hippocampal subfields, including the subicular complex, such as the parasubiculum, presubiculum, and subiculum, the CA regions, such as CA1, 2/3, 4, and fissure (hippocampal sulcus), the molecular layer (ML-DG) and granule cell layer of the dentate gyrus (CG-DG), as well as the transition areas, such as the hippocampal tail, fimbria, and hippocampal amygdala transition area (HATA; Iglesias et al., 2015). The hippocampal subfield segmentation was visually inspected using Freesurfer's Freeview (see Figure 1). The reliability of the hippocampal subfield segmentation has been evaluated in the previous study (Brown et al., 2020). Left and right hemispheres were summed together.

2.3 | CSF biomarkers

CSF biomarkers, such as amyloid-β42, t-tau, p-tau, were available in 972 subjects, including 247 HC subjects, 425 patients with s-MCI,

TABLE 1 Clinical and demographic characteristics of each clinical group

	HC	s-MCI	c-MCI	AD	Total
The number of subjects	421	557	241	304	1,523
Gender (M/F)	199/222	321/236	142/99	163/141	825/698
Baseline age, year	74.0 (5.8)	73.0 (7.8)	73.8 (7.1)	75.0 (7.7)	73.8 (7.2)
Education, year	16.5 (2.7)	15.8 (3.0)	16.0 (2.7)	15.0 (3.0)	15.9 (2.9)
MMSE	29.1 (1.1)	27.9 (1.7)	26.8 (1.8)	23.2 (2.1)	27.1 (2.7)
The number of follow-up scans	4.2 (2.2)	4.3 (1.9)	5.7 (1.7)	3.2 (1.1)	4.3 (2.0)
The duration of the first and last scans, year	2.6 (2.1)	2.1 (1.7)	3.3 (1.9)	1.2 (0.8)	2.1 (1.9)

Abbreviations: AD, Alzheimer's disease; c-MCI, converted MCI; HC, healthy control; MMSE, Mini-Mental State Examination; s-MCI, stable mild cognitive impairment.

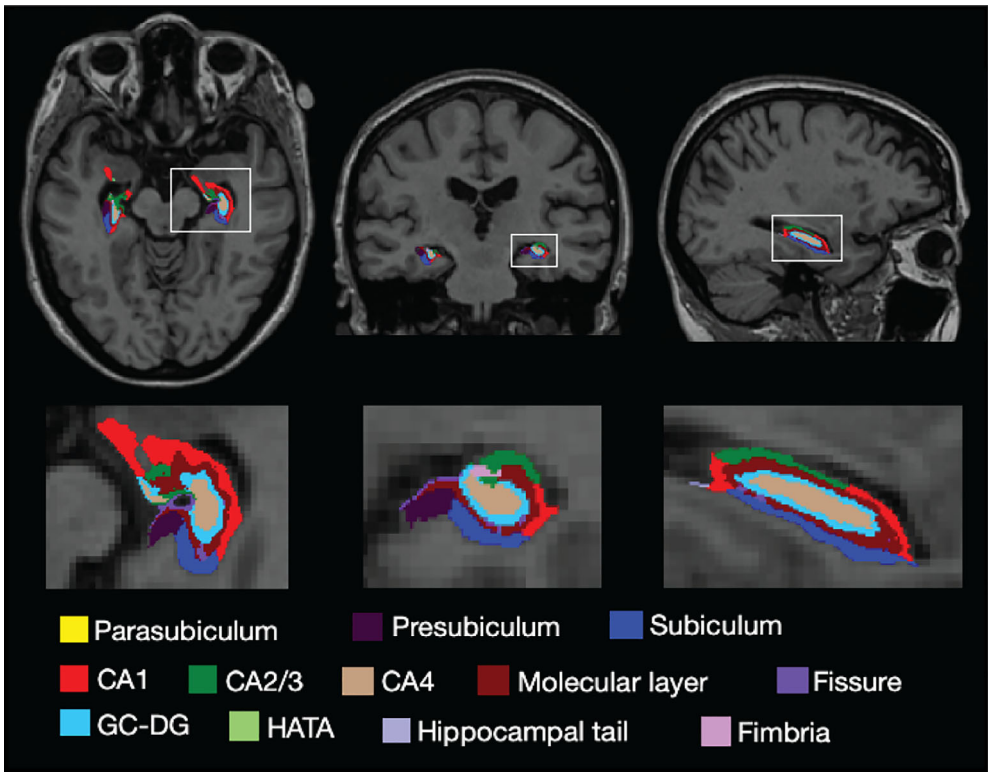

FIGURE 1 Illustration of the hippocampal subfields in the axial, coronal, and sagittal views. CA, cornu ammonis; DG, dentate gyrus; GC, granule cell; HATA, hippocampal amygdala transition area

82 patients with c-MCI, and 199 patients with AD. Among them, 514, 318, 96, 26, 8, and 9 subjects respectively had 1 ∼ 6 time points. One subject had eight-time points. Due to a limited number of subjects with CSF biomarkers at more than two-time points, this study computed the mean values of amyloid-β42, t-tau, and p-tau to represent the AD-related pathology.

2.4 | Cognitive measures

This study included cognitive data at all available time points. The scores from each cognitive test were combined into (a) memory domain from Rey Auditory Verbal Learning Test immediate and delayed scores; (b) language domain based on Boston Naming score; (c) visuospatial domain based on Clock Test score, and (d) attention/executive domain from Trail Making Test A score. All test scores were z-transformed and inverted if necessary in such a way that a lower value reflects worse cognitive performance. The z-transformed scores were then averaged to obtain the composite score for each of the four cognitive domains (ten Kate et al., 2018).

2.5 | Statistical analysis

We first examined the atrophy rate of each hippocampal subfield and compared it across the four groups using the linear mixed-effects model given below

$$\begin{aligned} Y_{ij} = {} & \beta_1 + \beta_2 \times t_{ij} + \beta_3 \times s\_MCI_i + \beta_4 \times s\_MCI_i \times t_{ij} + \beta_5 \times AD_i + \beta_6 \times AD_i \times t_{ij} \\ & + \beta_7 \times c\_MCI_i + \beta_8 \times c\_MCI_i \times t_{ij} + \beta_9 \times Education_i + \beta_{10} \\ & \times Gender_i + \beta_{11} \times BslAge_i + b_{1i} + b_{2i} * t_{ij} + e_{ij}. \end{aligned} \quad (1)$$

i and j denoted the indices of subjects and time points, respectively. Y_{ij} was the subfield volume ratio at time t_{ij} to the subfield volume averaged across all the time points of the ith subject. Hence, Y_{ij} was independent of the size of individual subfields and represented the atrophy rate of each subfield in terms of a percentage change of the subfield volume per year (Bernal-Rusiel, Greve, Reuter, Fischl, & Sabuncu, 2013; Bernal-Rusiel, Reuter, Greve, Fischl, & Sabuncu, 2013). For the sake of simplicity, we referred to the percentage of the atrophy rate of each subfield as "atrophy rate." We defined t_{ij} as the age at the jth follow-up scan from the age at the baseline scan ($BslAge_i$). This model also considered the interaction between diagnosis and time, assessing the atrophy rate of Y_{ij} in each disease group compared to HC. Gender and education were considered as covariates since the education level was a risk factor for AD (Qiu, Backman, Winblad, Aguero-Torres, & Fratiglioni, 2001) and the brain size of male and female was different (Ritchie et al., 2018). β_1 to β_{11} represented fixed effects, while b_{1i}, b_{2i} represented random effects that modeled the individual-specific intercept and atrophy rate of Y_{ij}. We then conducted F-tests and examined the pairwise group comparisons on the atrophy rate of Y_{ij}. For example, when β_2, β_4, or β_6 = 1, we examined the comparison of HC with s-MCI, AD, or c-MCI. We compared the atrophy rate between s-MCI and AD when setting β_4 = 1 and β_6 = −1. Bonferroni correction was used to correct statistical p-values (p < .05/13/3 = 0.00128, including 12 subfield structures and whole hippocampus, as well as three group comparisons, e.g., HC vs. s-MCI; s-MCI vs. c-MCI; c-MCI vs. AD). We further investigated whether the atrophy rate of specific hippocampal subfields was greater than that of the whole hippocampus via slope comparisons defined as

$$t = \frac{b_1 - b_2}{\sqrt{s_{b1}^2 + s_{b2}^2}}, df = n_1 + n_2 - 4.$$

b_1 and b_2 were the atrophy rates of a specific hippocampal subfield and the whole hippocampus, respectively. s_{b1} and s_{b2} were the standard errors of the atrophy rates of a specific hippocampal subfield and the whole hippocampus, respectively. And n_1 and n_2 were equal in our case and represented the number of subjects. The corresponding statistical results were reported after Bonferroni correction (p < .05/12 = 0.00417, 12 hippocampal subfields).

Second, we asked the question of whether the atrophy rate of specific hippocampal subfields was associated with the AD onset age in the c-MCI group. For this, we employed a linear regression model

$$Y_i = \beta_1 + \beta_2 \times Age_i + \beta_3 \times Education_i + \beta_4 \times Gender_i + e_i. \quad (2)$$

where the dependent variable, Y_i, was the atrophy rate of individual hippocampal subfields and the independent variable was the onset age of AD among the c-MCI participants. Gender and education were considered as covariates. We did not include random effects since this analysis examined one measurement (an atrophy rate of a specific hippocampal subfield) per subject and did not include multiple measurements per subject. Bonferroni correction was used to correct statistical p-values (p < .05/13 = 0.00385, including 12 subfield structures and whole hippocampus).

Likewise, we employed the same linear regression model as Equation (2) where the dependent variable was the atrophy rate of individual hippocampal subfields and the independent variable was CSF biomarkers in individual groups. Gender and education were considered as covariates. Bonferroni correction was used to correct statistical p-values (p < .05/13/3/4 = 0.00032, including 12 subfield structures and whole hippocampus, three CSF biomarkers, and four diagnostic groups).

Third, we examined the rate of cognitive declines in the four clinical groups and then its group comparisons. We employed the same linear mixed-effects models as those for the hippocampal subfield atrophy in Equation (1) where the dependent variable was the standardized cognitive score at a specific time of individual subjects. Statistical results were corrected via Bonferroni correction at a corrected p-value of .00417 (0.05/4/3 = 0.00417; four cognitive domains; three pairwise group comparisons, e.g., HC vs. s-MCI; s-MCI vs. c-MCI; c-MCI vs. AD).

Fourth, we employed linear regression to estimate the atrophy rate of the hippocampal subfields and the cognitive decline rate in

individuals. We then examined the relationship between the rate of cognitive decline and the atrophy rate of the hippocampal subfields via regression while gender and the years of education were considered as covariates. Statistical results were corrected via Bonferroni correction at a corrected *p*-value of .00092 (0.05/4/13 = 0.00092; four cognitive domains; 12 subfield structures and whole hippocampus).

3 | RESULTS

3.1 | Demographics

Table 1 lists the number of subjects, gender, years of education, and MMSE in the HC, s-MCI, c-MCI, and AD groups. The subjects in the four groups entered in the ADNI study around the same age. The proportion of males and females was different among the four groups (χ^2 = 13.03, p = .005). The four groups differed in the years of education ($F_{3,1519}$ = 13.8, p < .001).

3.2 | Atrophy of the hippocampal subfields

Figure 2 illustrates the atrophy rate of the hippocampal subfields in each group. In general, almost all the hippocampal subfields showed an increase in the atrophy rate from HC, s-MCI, c-MCI, to AD. Adjusting for gender and education, the group comparisons of the atrophy rate between HC and s-MCI and between s-MCI and c-MCI were statistically significant for most of the hippocampal subfields, except the HATA and fimbria (see corrected *p*-values in Table S1l). However, the atrophy rate of all the hippocampal subfields was statistically comparable between the c-MCI and AD groups. Likewise, the atrophy rate of the whole hippocampus was greater in the s-MCI group compared to the HC group (corrected p < .001) and in the c-MCI group compared to the s-MCI group (corrected p < .001), was comparable between the c-MCI and AD groups.

Compared to the whole hippocampus, the presubiculum and ML-DG showed a greater atrophy rate in all the four groups (corrected p < .001, Table S2). This pattern was also observed in the subiculum in the c-MCI group (corrected p = .038) and the fimbria in both the s-MCI and AD groups (corrected p < .001, Table S2).

3.3 | The correlation between the atrophy rate of the hippocampal subfields and the onset age of AD

Among the c-MCI patients, we further examined whether the atrophy rate of the hippocampal subfields predicted the onset age of AD. Figure 3 shows the correlation between the atrophy rate of the

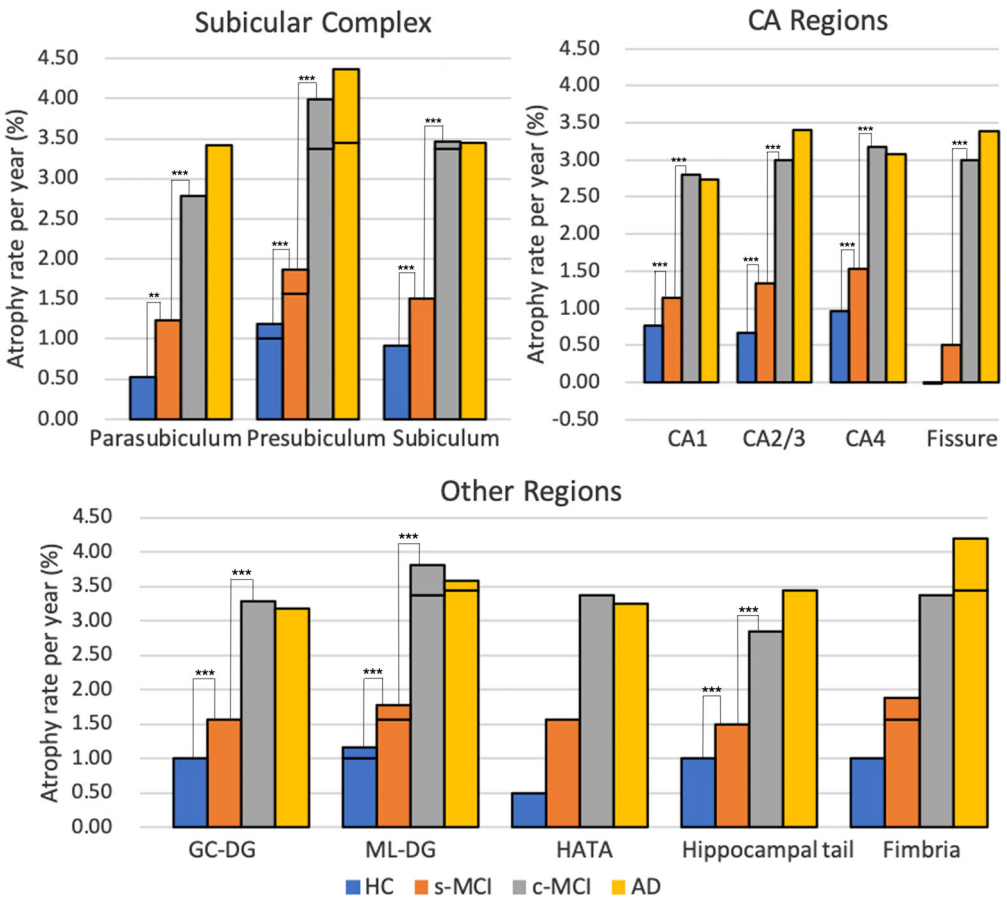

FIGURE 2 The atrophy rate of the hippocampal subfield volume ratio in each group. The black line indicates the atrophy rate of the whole hippocampus in the respective group. * indicates corrected *p*-values for the group comparisons. **, corrected p < .05; ***, corrected p < .01

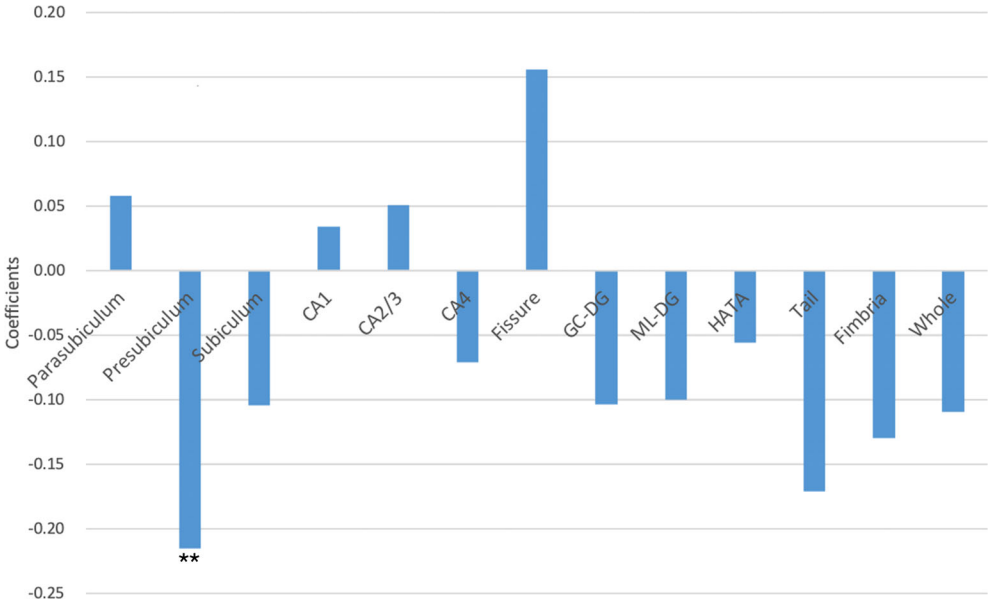

FIGURE 3 The correlation between the atrophy rate of the hippocampal subfields and the onset age of AD. **, corrected $p < .05$

hippocampal subfields and the onset age of AD, adjusting for gender and education. Among the 12 hippocampal subfields (Table S3), only the atrophy rate of the presubiculum was significantly correlated with the onset age of AD (corrected $p = .013$), suggesting that the larger atrophy rate of the presubiculum was associated with the earlier onset of AD.

3.4 | The correlation between the atrophy rate of the hippocampal subfields and CSF biomarkers

There was a significant effect of t-tau ($\beta = .43$, corrected $p = .006$) and p-tau ($\beta = .41$, corrected $p = .014$) levels on the atrophy rate of the presubiculum in the c-MCI group, with lower t-tau or p-tau levels corresponding to a higher atrophy rate of the presubiculum. There was no significant effect of amyloid-β42, or t-tau, or p-tau levels on the atrophy rates of the rest of the hippocampal subfields in any diagnostic groups (see Tables S4–S6).

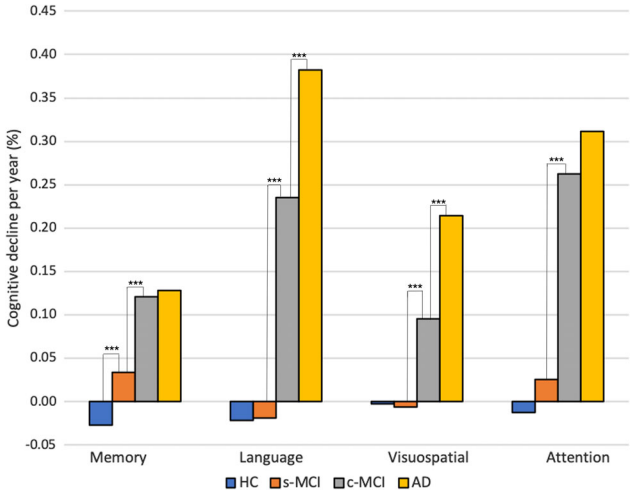

FIGURE 4 The rate of the cognitive decline in the healthy controls (HC), stable mild cognitive impairment (s-MCI), converted MCI (c-MCI), and Alzheimer's disease (AD) patients. ***, corrected $p < .01$

3.5 | Cognitive decline and its relationship with the atrophy rate of the hippocampal subfields

Figure 4 illustrates the decline rate of the four cognitive functions, including memory, language, visuospatial, and attention in the HC, s-MCI, c-MCI, and AD groups. Table S7 lists the statistical results for the group comparisons of the four cognitive measures. Compared to HC, s-MCI showed a greater memory decline (corrected $p < .001$). Compared to s-MCI, c-MCI had greater declines in all the four cognitive domains (all corrected $p < .001$). Compared to c-MCI, AD showed greater declines in the language (corrected $p < .001$) and visuospatial function (corrected $p = .003$). These results suggested the progressive cognitive decline from memory to the other three cognitive domains in the course of AD.

Figure 5 illustrates the correlation of the hippocampal subfield atrophy rates and cognitive declines in each group. In HC, a greater atrophy rate of the hippocampal tail was associated with a greater memory decline (corrected $p < .001$). In s-MCI, the greater atrophy rate of the presubiculum was associated with a greater memory decline (corrected $p < .001$). None of the hippocampal subfield atrophy rates was associated with memory decline in the c-MCI and AD groups (Table S8). Similarly, cognitive declines in the language and visuospatial functions were scarcely associated with the atrophy rates of the hippocampal subfields in each group (Tables S9 and S10). For instance, a greater decline of the language function was associated with the greater atrophy rates of the HATA in s-MCI, the subiculum, and CA4 in c-MCI (Table S9). A greater decline of the visuospatial

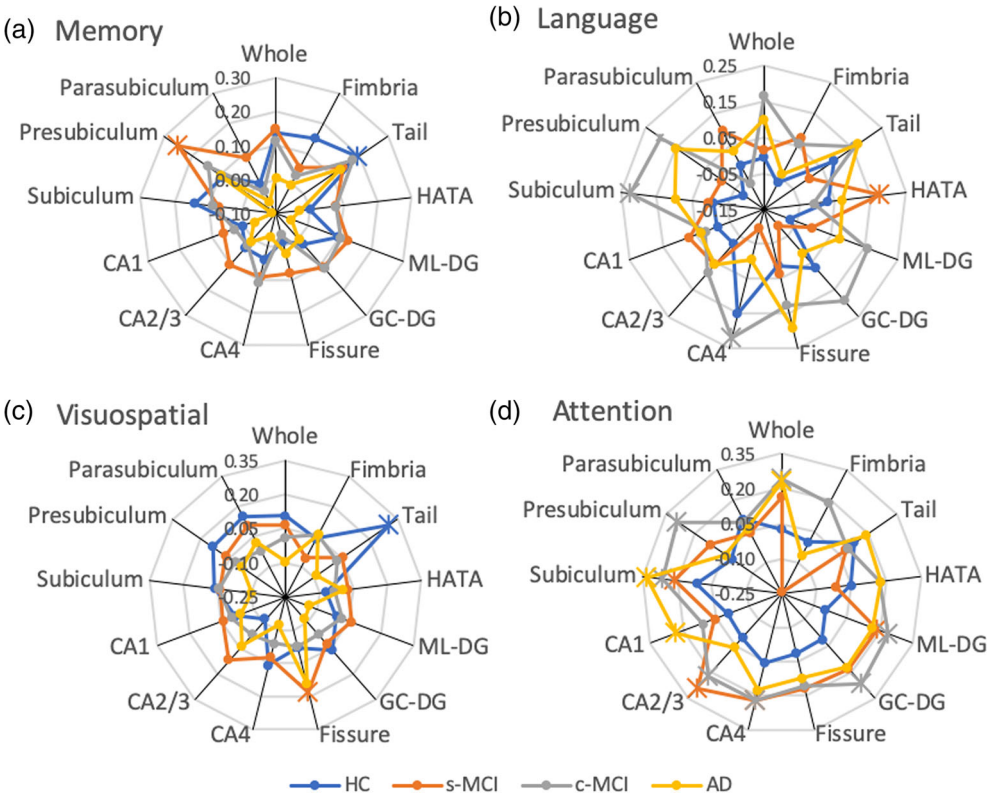

FIGURE 5 The correlation between the atrophy rate of the hippocampal subfields and the cognitive decline rate in memory (a), language (b), visuospatial (c), and attention (d). * corrected *p*-value <.05

function was associated with a greater atrophy rate of the hippocampal tail in HC and the fissure in s-MCI (Table S10). Nevertheless, the s-MCI and c-MCI groups showed a positive relationship of the decline in the attention function with the atrophy rate of most of the subicular complex and CA regions, as well as the DG (Table S11). These results provided the spatial correlation map of the hippocampus with the cognitive decline in the cognitively normal aging, MCI, and AD.

4 | DISCUSSION

This study included subjects in the cognitively normal, MCI, and AD groups whose clinical stage was stable over a long period. Hence, our findings provided insights into the involvement of the hippocampal subfields in stable cognitively normal aging, MCI, and AD. All the hippocampal subfields accelerated their atrophy rate from cognitively normal aging to stable MCI and AD, which is consistent with the previous findings (Parker et al., 2019). The presubiculum, ML-DG, and fimbria showed greater atrophy beyond the whole hippocampus in the HC, s-MCI, and AD groups and corresponded to a greater decline of memory and attention in the s-MCI group. Moreover, the higher atrophy rates of the subiculum and CA2/3, CA4 were also associated with a greater decline in attention in the s-MCI group. These findings suggested that the hippocampal subfields may not be equally impacted by normal aging, MCI and AD and their atrophy were selectively associated with declines in specific cognitive domains (Apostolova et al., 2006; Braak et al., 2006; Braak & Braak, 1997; Kerchner et al., 2012; La Joie et al., 2013).

There is evidence to suggest preferential atrophy of specific subfields, especially the CA1 and the subicular complex in AD (Apostolova et al., 2006; Apostolova et al., 2010; Blanken et al., 2017; La Joie et al., 2013; Mueller et al., 2010). Interestingly, our study suggested that the presubiculum atrophy was associated with CSF tau levels and corresponded to the onset age of AD and a decline in attention in patients with c-MCI. The presubiculum volume loss was found in patients with posterior cortex atrophy of early onset AD (Parker et al., 2019). The presubiculum anatomically connects with the posterior cortex and receives anatomical projections from the parietal and occipital cortex (Cavada & Goldman-Rakic, 1989; Parker et al., 2019; Parker et al., ; Seltzer & Pandya, 1984; Seltzer & Van Hoesen, 1979; Vogt & Miller, 1983). Tau becomes abnormally phosphorylated and aggregates into neurofibrillary tangles (NFTs). NFT affected neurons may result in disconnection and deafferentation of critical neural communication between the presubiculum and parieto-occipital cortex and thus is likely to (Duyckaerts, Delatour, & Potier, 2009; Hyman, Hoesen, & Damasio, 1990) contribute to the defects in attention in patients with c-MCI.

There is great emphasis on the role of the hippocampus and its subfields in memory (Barry, Clark, & Maguire, 2020; Bartsch, Dohring, Rohr, Jansen, & Deuschl, 2011; Bennett, Stark, & Stark, 2018; Chadwick, Bonnici, & Maguire, 2014; Dimsdale-Zucker, Ritchey, Ekstrom, Yonelinas, & Ranganath, 2018; Perez-Cruz et al., 2011; Mueller, Chao, Berman, & Weiner, 2011; Zheng et al., 2018). Our study also demonstrated the presubiculum atrophy corresponding to memory decline in patients with s-MCI. Beyond memory, our study provided strong evidence on the involvement of the subicular complex, CA2,3,4, and DG

regions in the progressive decline of attention in patients with s-MCI or c-MCI or AD. The molecular layer of the DG receives sensory information from the unimodal and polymodal cortex via the entorhinal cortex and projects to the CA2/3, then to the CA1. While the subicular complex, CA1, CA2/3, and DG are implicated in memory encoding (Acsády & Káli, 2007; Hasselmo, 2005; Travis et al., 2014), consolidation (Hunsaker & Kesner, 2008; Nakazawa et al., 2004; Wan et al., 1999), and retrieval (Hasselmo, 2005), they have been also suggested to play a role in attention (Aly & Turk-Browne, 2015). Memory can serve to guide attention (Stokes Mark, 2012) and attention is crucial for the encoding and retrieval of memory (Chun & Turk-Browne, 2007; Hardt & Nadel, 2009). The discriminate activity patterns in the CA2/3 and DG for different motivational states correlate with associative memory (Wolosin, Zeithamova, & Preston, 2013). The CA2/3 and DG activity was found to be associated with behavior in an online attention task (Wolosin et al., 2013). Our results support a significant association of the atrophy of specific subicular, CA, and DG subfields with attention decline as a non-memory cognitive impairment in patients with s-MCI and c-MCI.

This study had several advantages and limitations. This study incorporated all structural MRI, CSF biomarkers, and cognition data available in ADNI to maximize the potential for exploring the roles of the atrophy of hippocampal subfields in different stages of AD and their relations with CSF biomarkers and cognitive decline over the period of 15 years. Since the sample size of the study was large and all time-points were included, our study may provide more reliable findings on the hippocampal subfields in AD. Due to a limited number of subjects with multiple time-point CSF biomarkers, our study was not able to assess the changes of CSF biomarkers over time and their relationship with the hippocampal subfield atrophy in the course of AD. Moreover, the T1-weighted MRI in the ADNI study had relatively large spatial resolution ($\geq$1 mm^3), which may not have enough spatial resolution and image contrast to see and/or identify small hippocampal subfields, such as the ML. In this study, we combined the ML with CA4 as suggested in (Iglesias et al., 2015), repeated the analysis, and showed the findings reported here remained the same (see Section C in the Data S1). Future studies should consider fine spatial resolution and multi-modal MRI acquisition (T1- and T2-weighted images). Last but not least, the images in the ADNI study were acquired using 1.5T and 3T scanners. We further repeated analysis while applying ComBat (Pomponio et al., 2020) to correct potential effects due to scanner field strength and reported the findings in Tables S12–S21. Again, our findings remained largely unchanged or became marginally significant, suggesting the robustness of the findings reported in this study. Nevertheless, longitudinal MRI studies always face challenges of changes in image acquisition due to software upgrade, field strength, scanner upgrade, and et al. Hence, a large study sample is needed to overcome potential effects due to such factors.

In conclusion, this study provided reliable evidence on the spatial correlation maps of the hippocampal subfields with CSF biomarkers and cognition in cognitively normal aging, stable and converted MCI, and AD over time. Our study highlighted the presubiculum atrophy as a potential surrogate marker in the prediction of the AD onset age and in the link with tau pathology and attention decline in the conversion from MCI to AD. Our findings provided important information for clinical prognosis and monitoring the progression of AD.

DISCLOSURES AND ACKNOWLEDGMENTS

This work was supported by the Singapore Ministry of Education and NUS Institute of Data Science, Singapore. This research/project is supported by the National Research Foundation, Singapore under its AI Singapore Programme (AISG Award No: AISG-GC-2019-002). Additional funding is provided by the Singapore Ministry of Education (Academic research fund Tier 1) and NUS Institute of Data Science. This research was also supported by the A*STAR Computational Resource Centre through the use of its high-performance computing facilities.

Data collection and sharing for this project was funded by the Alzheimer's Disease Neuroimaging Initiative (ADNI; National Institutes of Health Grant U01 AG024904) and DOD ADNI (Department of Defense award number W81XWH-12-2-0012). ADNI is funded by the National Institute on Aging, the National Institute of Biomedical Imaging and Bioengineering, and through generous contributions from the following: AbbVie, Alzheimer's Association; Alzheimer's Drug Discovery Foundation; Araclon Biotech; BioClinica, Inc.; Biogen; Bristol-Myers Squibb Company; CereSpir, Inc.; Cogstate; Eisai Inc.; Elan Pharmaceuticals, Inc.; Eli Lilly and Company; EuroImmun; F. Hoffmann-La Roche Ltd and its affiliated company Genentech, Inc.; Fujirebio; GE Healthcare; IXICO Ltd.; Janssen Alzheimer Immunotherapy Research & Development, LLC.; Johnson & Johnson Pharmaceutical Research & Development LLC.; Lumosity; Lundbeck; Merck & Co., Inc.; Meso Scale Diagnostics, LLC.; NeuroRx Research; Neurotrack Technologies; Novartis Pharmaceuticals Corporation; Pfizer Inc.; Piramal Imaging; Servier; Takeda Pharmaceutical Company; and Transition Therapeutics. The Canadian Institutes of Health Research is providing funds to support ADNI clinical sites in Canada. Private sector contributions are facilitated by the Foundation for the National Institutes of Health (www.fnih.org). The grantee organization is the Northern California Institute for Research and Education, and the study is coordinated by the Alzheimer's Therapeutic Research Institute at the University of Southern California. ADNI data are disseminated by the Laboratory for Neuro Imaging at the University of Southern California.

DATA AVAILABILITY STATEMENT

The data used in this article is available in the ADNI website (http://www.adni-info.org).

ORCID

Anqi Qiu https://orcid.org/0000-0002-0215-6338

REFERENCES

Acsády, L., & Káli, S. (2007). Models, structure, function: The transformation of cortical signals in the dentate gyrus. *Progress in Brain Research*, *163*, 577–599.

Adler, D. H., Wisse, L. E. M., Ittyerah, R., Pluta, J. B., Ding, S.-L., Xie, L., … Yushkevich, P. A. (2018). Characterizing the human hippocampus in aging and Alzheimer's disease using a computational atlas derived from ex vivo MRI and histology. *Proceedings of the National Academy of Sciences of the United States of America*, *115*, 4252–4257.

Aggleton, J. P., & Christiansen, K. (2015). Chapter 4—The subiculum: The heart of the extended hippocampal system. In S. O'Mara & M. Tsanov (Eds.), *Progress in brain research* (pp. 65–82). Amsterdam, The Netherlands: Elsevier.

Aly, M., & Turk-Browne, N. B. (2015). Attention stabilizes representations in the human hippocampus. *Cerebral Cortex*, *26*, 783–796.

Apostolova, L. G., Dutton, R. A., Dinov, I. D., Hayashi, K. M., Toga, A. W., Cummings, J. L., & Thompson, P. M. (2006). Conversion of mild cognitive impairment to Alzheimer Disease predicted by hippocampal atrophy maps. *Archives of Neurology (Chicago)*, *63*, 693–699.

Apostolova, L. G., Mosconi, L., Thompson, P. M., Green, A. E., & Leon, M. J. D. (2010). Subregional hippocampal atrophy predicts Alzheimer's dementia in the cognitively normal. *Neurobiology of Aging*, *31*, 1077–1088.

Apostolova, L. G., Zarow, C., Biado, K., Hurtz, S., Boccardi, M., Somme, J., … Watson, C. (2015). Relationship between hippocampal atrophy and neuropathology markers: A 7T MRI validation study of the EADC-ADNI Harmonized Hippocampal Segmentation Protocol. *Alzheimer's & Dementia*, *11*, 139–150.

Barry, D. N., Clark, I. A., & Maguire, E. A.(2020). The relationship between hippocampal subfield volumes and autobiographical memory persistence. *Hippocampus*.

Bartsch, T., Dohring, J., Rohr, A., Jansen, O., & Deuschl, G. (2011). CA1 neurons in the human hippocampus are critical for autobiographical memory, mental time travel, and autonoetic consciousness. *Proceedings of the National Academy of Sciences*, *108*(42), 17562–17567.

Bennett, I. J., Stark, S. M., & Stark, C. E. L. (2018). Recognition memory dysfunction relates to hippocampal subfield volume: A study of cognitively normal and mildly impaired older adults. *The Journals of Gerontology: Series B*, *74*, 1132–1141.

Bernal-Rusiel, J. L., Greve, D. N., Reuter, M., Fischl, B., & Sabuncu, M. R. (2013). Statistical analysis of longitudinal neuroimage data with linear mixed effects models. *NeuroImage*, *66*, 249–260.

Bernal-Rusiel, J. L., Reuter, M., Greve, D. N., Fischl, B., & Sabuncu, M. R. (2013). Spatiotemporal linear mixed effects modeling for the mass-univariate analysis of longitudinal neuroimage data. *NeuroImage*, *81*, 358–370.

Blanken, A. E., Hurtz, S., Zarow, C., Biado, K., Honarpisheh, H., Somme, J., … Apostolova, L. G. (2017). Associations between hippocampal morphometry and neuropathologic markers of Alzheimer's disease using 7 T MRI. *NeuroImage: Clinical*, *15*, 56–61.

Braak, E., & Braak, H. (1997). Alzheimer's disease: Transiently developing dendritic changes in pyramidal cells of sector CA1 of the Ammon's horn. *Acta Neuropathologica*, *93*, 323–325.

Braak, H., Alafuzoff, I., Arzberger, T., Kretzschmar, H., & Del Tredici, K. (2006). Staging of Alzheimer disease-associated neurofibrillary pathology using paraffin sections and immunocytochemistry. *Acta Neuropathologica*, *112*, 389–404.

Braak, H., & Braak, E. (1995). Staging of alzheimer's disease-related neurofibrillary changes. *Neurobiology of Aging*, *16*, 271–278.

Broadhouse, K. M., Mowszowski, L., Duffy, S., Leung, I., Cross, N., Valenzuela, M. J., & Naismith, S. L. (2019). Memory performance correlates of hippocampal subfield volume in mild cognitive impairment subtype. *Frontiers in Behavioral Neuroscience*, *13*, 259.

Brown, E. M., Pierce, M. E., Clark, D. C., Fischl, B. R., Iglesias, J. E., Milberg, W. P., … Salat, D. H. (2020). Test-retest reliability of FreeSurfer automated hippocampal subfield segmentation within and across scanners. *NeuroImage (Orlando, Fla.)*, *210*, 116563.

Brunton, S., Ginestet, C., Lovestone, S., Muehlboeck, S., & Simmons, A. (2011). P4-351: Longitudinal volume changes of the hippocampus, parahippocampus and entorhinal cortex improve the prediction of conversion from MCI to Alzheimer's disease. *Alzheimer's & Dementia*, *7*, e34–e35.

Cavada, C., Goldman-Rakic, P.S., 1989. Posterior parietal cortex in rhesus monkey: II. Evidence for segregated corticocortical networks linking sensory and limbic areas with the frontal lobe. *Journal of Comparative Neurology* (1911) *287*, 422–445.

Chadwick, M. J., Bonnici, H. M., & Maguire, E. A. (2014). CA3 size predicts the precision of memory recall. Proceedings of the National Academy of Sciences. *PNAS*, *111*, 10720–10725.

Chun, M. M., & Turk-Browne, N. B. (2007). Interactions between attention and memory. *Current Opinion in Neurobiology*, *17*, 177–184.

Dimsdale-Zucker, H. R., Ritchey, M., Ekstrom, A. D., Yonelinas, A. P., & Ranganath, C. (2018). CA1 and CA3 differentially support spontaneous retrieval of episodic contexts within human hippocampal subfields. *Nature Communications*, *9*, 294.

Duyckaerts, C., Delatour, B., & Potier, M. C. (2009). Classification and basic pathology of Alzheimer disease. *Acta Neuropathologica*, *118*, 5–36.

Gerischer, L. M., Fehlner, A., Köbe, T., Prehn, K., Antonenko, D., Grittner, U., … Flöel, A. (2018). Combining viscoelasticity, diffusivity and volume of the hippocampus for the diagnosis of Alzheimer's disease based on magnetic resonance imaging. *NeuroImage: Clinical*, *18*, 485–493.

Hardt, O., & Nadel, L. (2009). Cognitive maps and attention. *Progress in Brain Research*, *176*, 181–194.

Hasselmo, M. E. (2005). The role of hippocampal regions CA3 and CA1 in matching entorhinal input with retrieval of associations between objects and context: Theoretical comment on lee et al. (2005). *Behavioral Neuroscience*, *119*, 342–345.

Hunsaker, M. R., & Kesner, R. P. (2008). Evaluating the differential roles of the dorsal dentate gyrus, dorsal CA3, and dorsal CA1 during a temporal ordering for spatial locations task. *Hippocampus*, *18*, 955–964.

Hyman, B. T., Hoesen, G. W. V., & Damasio, A. R. (1990). Memory-related neural systems in Alzheimer's disease: An anatomic study. *Neurology*, *40*, 1721–1730.

Iglesias, J. E., Augustinack, J. C., Nguyen, K., Player, C. M., Player, A., Wright, M., … Alzheimer's Disease Neuroimaging, I. (2015). A computational atlas of the hippocampal formation using ex vivo, ultra-high resolution MRI: Application to adaptive segmentation of in vivo MRI. *NeuroImage*, *115*, 117–137.

Jack, C. R. J., Bernstein, M. A., Fox, N. C., Thompson, P., Alexander, G., Harvey, D., … Study, A. (2008). The Alzheimer's Disease Neuroimaging Initiative (ADNI): MRI methods. *Journal of Magnetic Resonance Imaging*, *27*, 685–691.

Kerchner, G. A., Deutsch, G. K., Zeineh, M., Dougherty, R. F., Saranathan, M., & Rutt, B. K. (2012). Hippocampal CA1 apical neuropil atrophy and memory performance in Alzheimer's disease. *NeuroImage (Orlando, Fla.)*, *63*, 194–202.

La Joie, R., Perrotin, A., de La Sayette, V., Egret, S., Doeuvre, L., Belliard, S., … Chételat, G. (2013). Hippocampal subfield volumetry in mild cognitive impairment, Alzheimer's disease and semantic dementia. *NeuroImage: Clinical*, *3*, 155–162.

Laakso, M. P., Frisoni, G. B., Könönen, M., Mikkonen, M., Beltramello, A., Geroldi, C., … Aronen, H. J. (2000). Hippocampus and entorhinal cortex in frontotemporal dementia and Alzheimer's disease: A morphometric MRI study. *Biological Psychiatry*, *47*, 1056–1063.

Laakso, M. P., Soininen, H., Partanen, K., Lehtovirta, M., Hallikainen, M., Hänninen, T., … Riekkinen, P. J. (1998). MRI of the hippocampus in Alzheimer's Disease: Sensitivity, specificity, and analysis of the incorrectly classified subjects. *Neurobiology of Aging*, *19*, 23–31.

Lehtovirta, M., Laakso, M. P., Soininen, H., Helisalmi, S., Mannermaa, A., Helkala, E. L., … Riekkinen, P. J. (1995). Volumes of hippocampus, amygdala and frontal lobe in Alzheimer patients with different apolipoprotein E genotypes. *Neuroscience*, *67*, 65–72.

Likeman, M., Anderson, V. M., Stevens, J. M., Waldman, A. D., Godbolt, A. K., Frost, C., … Fox, N. C. (2005). Visual assessment of atrophy on magnetic resonance imaging in the diagnosis of pathologically confirmed young-onset dementias. *Archives of Neurology*, *62*, 1410–1415.

Mueller, S. G., Chao, L. L., Berman, B., & Weiner, M. W. (2011). Evidence for functional specialization of hippocampal subfields detected by MR subfield volumetry on high resolution images at 4T. *NeuroImage*, *56*, 851–857.

Mueller, S. G., Schuff, N., Yaffe, K., Madison, C., Miller, B., & Weiner, M. W. (2010). Hippocampal atrophy patterns in mild cognitive impairment and Alzheimer's disease. *Human Brain Mapping*, *31*, 1339–1347.

Nakazawa, K., McHugh, T. J., Wilson, M. A., & Tonegawa, S. (2004). NMDA receptors, place cells and hippocampal spatial memory. *Nature Reviews. Neuroscience*, *5*, 361–372.

Ogawa, M., Sone, D., Beheshti, I., Maikusa, N., Okita, K., Takano, H., & Matsuda, H. (2019). Association between subfield volumes of the medial temporal lobe and cognitive assessments. *Heliyon*, *5*, e01828.

Parker, T. D., Slattery, C. F., Yong, K. X. X., Nicholas, J. M., Paterson, R. W., Foulkes, A. J. M., … Crutch, S. J. (2019). Differences in hippocampal subfield volume are seen in phenotypic variants of early onset Alzheimer's disease. *NeuroImage: Clinical*, *21*, 101632.

Perez-Cruz, C., Nolte, M. W., van Gaalen, M. M., Rustay, N. R., Termont, A., Tanghe, A., … Ebert, U. (2011). Reduced spine density in specific regions of CA1 pyramidal neurons in two transgenic mouse models of Alzheimer's disease. *The Journal of Neuroscience: The Official Journal of the Society for Neuroscience*, *31*, 3926–3934.

Pomponio, R., Erus, G., Habes, M., Doshi, J., Srinivasan, D., Mamourian, E., … Davatzikos, C. (2020). Harmonization of large MRI datasets for the analysis of brain imaging patterns throughout the lifespan. *NeuroImage*, *208*, 116450.

Qiu, C., Backman, L., Winblad, B., Aguero-Torres, H., & Fratiglioni, L. (2001). The influence of education on clinically diagnosed dementia incidence and mortality data from the Kungsholmen Project. *Archives of Neurology*, *58*, 2034–2039.

Ritchie, S. J., Cox, S. R., Shen, X., Lombardo, M. V., Reus, L. M., Alloza, C., … Deary, I. J. (2018). Sex differences in the adult human brain: Evidence from 5216 UKBiobank participants. *Cerebral Cortex*, *28*, 2959–2975.

Seltzer, B., & Pandya, D. N. (1984). Further observations on parieto-temporal connections in the rhesus monkey. *Experimental Brain Research*, *55*, 301–312.

Seltzer, B., & Van Hoesen, G. W. (1979). A direct inferior parietal lobule projection to the presubiculum in the rhesus monkey. *Brain Research*, *179*, 157–161.

Small, S. A., Schobel, S. A., Buxton, R. B., Witter, M. P., & Barnes, C. A. (2011). A pathophysiological framework of hippocampal dysfunction in ageing and disease. *Nature Reviews. Neuroscience*, *12*, 585–601.

Stokes Mark, G. (2012). Long-term memory prepares neural activity for perception. *Proceedings of the National Academy of Sciences of the United States of America*, *109*(6), E360–E367.

Strawbridge, R. J., Ward, J., Lyall, L. M., Tunbridge, E. M., Cullen, B., Graham, N., … Smith, D. J. (2018). Genetics of self-reported risk-taking behaviour, trans-ethnic consistency and relevance to brain gene expression. *Translational Psychiatry*, *8*, 178.

ten Kate, M., Dicks, E., Visser, P. J., van der Flier, W. M., Teunissen, C. E., Barkhof, F., … Alzheimer's Disease Neuroimaging, I. (2018). Atrophy subtypes in prodromal Alzheimer's disease are associated with cognitive decline. *Brain*, *141*, 3443–3456.

Travis, S. G., Huang, Y., Fujiwara, E., Radomski, A., Olsen, F., Carter, R., … Malykhin, N. V. (2014). High field structural MRI reveals specific episodic memory correlates in the subfields of the hippocampus. *Neuropsychologia*, *53*, 233–245.

Vogt, B. A., & Miller, M. W. (1983). Cortical connections between rat cingulate cortex and visual, motor, and postsubicular cortices. *Journal of Comparative Neurology* (1911), *216*, 192–210.

Wan, H., Aggleton, J. P., & Brown, M. W. (1999). Different contributions of the hippocampus and perirhinal cortex to recognition memory. *The Journal of Neuroscience*, *19*, 1142–1148.

Wolosin, S. M., Zeithamova, D., & Preston, A. R. (2013). Distributed hippocampal patterns that discriminate reward context are associated with enhanced associative binding. *Journal of Experimental Psychology General*, *142*, 1264–1276.

Zheng, F., Cui, D., Zhang, L., Zhang, S., Zhao, Y., Liu, X., … Qiu, J. (2018). The volume of hippocampal subfields in relation to decline of memory recall across the adult lifespan. *Frontiers in Aging Neuroscience*, *10*, 320.

SUPPORTING INFORMATION

Additional supporting information may be found online in the Supporting Information section at the end of this article.

How to cite this article: Liu G, Liu C, Qiu A, the Alzheimer's Disease Neuroimaging Initiative. Spatial correlation maps of the hippocampus with cerebrospinal fluid biomarkers and cognition in Alzheimer's disease: A longitudinal study. *Hum Brain Mapp*. 2021;42:2931–2940. https://doi.org/10.1002/hbm.25414